

# An Improved Numerical Method for Predicting Intermetallic Layer Thickness Developed during the Formation of Solder Joints on Cu Substrates

S. CHADA,<sup>1,2</sup> W. LAUB,<sup>1,3</sup> R.A. FOURNELLE,<sup>1</sup> and D. SHANGGUAN<sup>4</sup>

1.—Materials Science and Engineering Program, Marquette University, Milwaukee, WI 53201. 2.—Presently at Soletron Corporation, 727 Gibraltar Drive, Milpitas, CA 95035. 3.—Presently at Soletron GmbH, Soletronstr. 2, 71083 Herrenberg, Germany. 4.—Visteon Automotive Systems, Ford Motor Company, 17000 Rotunda Drive, Dearborn, MI 48121

An improved numerical method has been developed for calculating the thickness of intermetallic layers formed between Cu substrates and solders during the soldering process. The improved method takes into account intermetallic dissolution during heating and intermetallic precipitation during cooling and requires as input (1) the temperature-time profile for the soldering process, (2) the experimentally determined isothermal growth parameters for the growth of the intermetallic layer into Cu saturated molten solder, (3) the experimentally determined Nernst-Brunner parameters for the dissolution of Cu into molten solder, (4) the experimentally determined solubility of Cu in molten solder and (5) assumptions about the thickness of the boundary layer in the liquid ahead of the growing intermetallic. Calculations show that the improved method predicts intermetallic growth between Cu substrates and 96.5Sn-3.5Ag solder during reflow soldering better than a previously developed method, which did not take into account dissolution during heating and precipitation during cooling. Calculations further show that dissolution has a significant effect on growth, while precipitation does not.

**Key words:** Cu-Sn intermetallics, Cu substrate, intermetallic compound growth, Sn-Ag solder

## INTRODUCTION

In an earlier paper<sup>1</sup> a numerical method for predicting the thickness of the intermetallic layer developed during reflow soldering of Sn containing solders on Cu substrates was presented. This method required as input the temperature-time profile of the solder while it is in the liquid state on the Cu substrate and an experimentally determined equation or equations describing the isothermal growth of the intermetallic layer. The method basically involved dividing up the temperature-time profile into a large number of equal time intervals and then treating the growth in each interval as isothermal. The total layer thickness at any time during the reflow cycle was taken to be the sum of the individual increments of growth during these isothermal intervals. This method underestimated somewhat the thickness of intermetallic layers developed during the reflow of Sn-Pb-Ag solder on Cu. One reason for this may be that the method did not

take into account dissolution of intermetallic during the heating part of the reflow cycle and precipitation of intermetallic during the cooling part. Schaefer et al.<sup>2</sup> have clearly shown that isothermal growth of intermetallic between molten Sn-Pb-Ag solder and a Cu substrate is affected by dissolution. It is the objective of this paper to improve on the numerical technique by taking into account (1) the intermetallic dissolution occurring simultaneously with intermetallic growth during the heating and cooling parts of the reflow cycle up to saturation of the solder with Cu and (2) intermetallic precipitation occurring simultaneously with growth during the cooling part of the cycle after saturation.

## NUMERICAL METHOD

Like the numerical method presented previously<sup>1</sup> the method presented here requires as input the relevant temperature-time profile (Fig. 1) of the soldering process and an equation for the isothermal thickening of the intermetallic layer as a function of time. However, the improved method also requires

(Received March 3, 1999; accepted May 6, 1999)

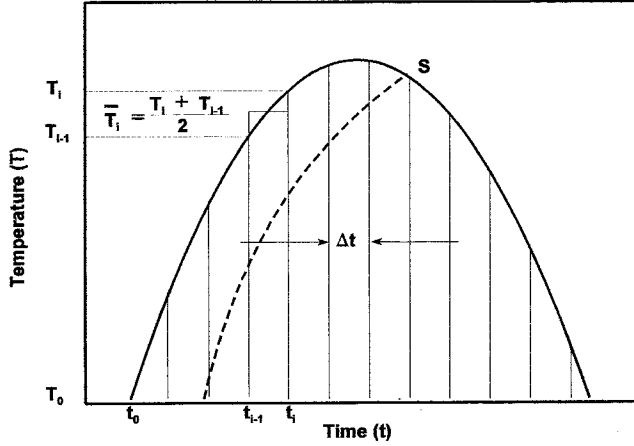


Fig. 1. Schematic diagram of the reflow portion of the temperature-time profile of a reflow oven (solid line) broken down into small isothermal increments of equal time  $\Delta t$ . The dashed line represents the solubility temperature corresponding to the solute content of the solder. The point S indicates the temperature and time at which the molten solder reaches saturation.

experimentally determined equations for the isothermal dissolution of the intermetallic layer which occurs simultaneously with layer growth during the heating and cooling part of the reflow cycle up to the point S in Fig. 1. At this point the solder becomes saturated with solute (Cu in this study). It also requires a method for taking into account any precipitation of solute as intermetallic ( $\eta$  in this study) during cooling from the point of saturation until solidification is complete. In this study the dissolution effect is taken into account using experimentally determined Nernst-Brunner equation parameters in conjunction with an experimentally determined solubility limit curve for Cu in molten solder. The precipitation effect is taken into account by employing an established equation for isothermal growth of a phase into a supersaturated solution.

Following the work of Schaefer et al.<sup>1</sup> the temperature (T)-time (t) profile is divided into equal time intervals  $\Delta t$ . Growth and dissolution or precipitation of intermetallic during each interval is then treated isothermally at an average temperature

$$\bar{T}_i = \frac{T_i + T_{i-1}}{2} \quad (1)$$

Here  $i$  denotes the  $i^{\text{th}}$  interval. The increase of intermetallic thickness  $\Delta x_i$  during each interval is taken to be

$$\Delta x_i = \Delta x_i^g - \Delta x_i^d \quad (2a)$$

for growth prior to saturation (Point S in Fig. 1) and

$$\Delta x_i = \Delta x_i^g + \Delta x_i^p \quad (2b)$$

for growth after saturation. Here  $\Delta x_i^g$  is the increment of growth associated with the isothermal growth of the intermetallic layer into a saturated liquid,  $\Delta x_i^d$  is the increment of intermetallic dissolution into a less than saturated liquid, and  $\Delta x_i^p$  is the incremental increase in thickness resulting from precipitation

onto the layer from supersaturated liquid solution.

The total layer thickness  $x_i$  after the  $i^{\text{th}}$  interval is thus given by

$$x_i = x_{i-1} + \Delta x_i^g - \Delta x_i^d \quad (3a)$$

for growth prior to saturation and by

$$x_i = x_{i-1} + \Delta x_i^g + \Delta x_i^p \quad (3b)$$

for growth after saturation. How the individual terms in the above equations are determined is described below.

As in the work of Schaefer et al.<sup>1</sup> the increment of growth  $\Delta x_i^g$  is taken to be the average growth rate  $\bar{v}_i^g$  in this interval times its width  $\Delta t$ . The value of  $\bar{v}_i^g$  is obtained from an experimentally determined equation for the isothermal growth or thickening of the intermetallic layer into a saturated liquid. This is usually given by a power law relationship of the form,

$$x(T,t) = kt^n \quad (4)$$

where  $x$  is the thickness of the intermetallic layer and  $k$  and  $n$  are experimentally determined parameters. Here

$$k = k^0 \exp\left(-\frac{Q_g}{RT}\right) \quad (5)$$

where  $k^0$  and  $Q_g$ , the apparent activation energy for layer growth, are also experimentally established parameters.

To get the increment of growth  $\Delta x_i^g$  during the  $i^{\text{th}}$  interval one first differentiates Eq. 4 to get the average growth or thickening rate,

$$v(T,t) = knt^{n-1} \quad (6)$$

To get the growth rate in the  $i^{\text{th}}$  interval one evaluates  $v$  for an equivalent time  $t_i^e$  associated with the interval. This equivalent time is taken as the time for the isothermal growth of a layer of thickness  $x_{i-1}$  at  $\bar{T}_i$  plus  $\Delta t/2$ . As explained by Schaefer et al.<sup>1</sup> this is given by

$$t_i^e = \left(\frac{x_{i-1}}{k_i}\right)^{\frac{1}{n}} + \frac{\Delta t}{2} \quad (7)$$

Combining Eqs. 6 and 7 one then gets

$$\bar{v}_i^g = nk_i \left[ \left(\frac{x_{i-1}}{k_i}\right)^{\frac{1}{n}} + \frac{\Delta t}{2} \right]^{n-1} \quad (8)$$

for the thickening rate during the  $i^{\text{th}}$  interval. Thus, the increase in layer thickness  $\Delta x_i$  during this interval is given by

$$\Delta x_i^g = nk_i \left[ \left(\frac{x_{i-1}}{k_i}\right)^{\frac{1}{n}} + \frac{\Delta t}{2} \right]^{n-1} \Delta t \quad (9)$$

The increment of layer dissolution  $\Delta x_i^d$  during the  $i$ th interval prior to saturation is calculated by determining the amount of solute (Cu) dissolved during the interval using an experimentally determined Nernst-Brunner equation for dissolution. Knowing the amount of solute dissolved, the volume of the molten solder, and the substrate contact area and assuming that dissolution results exclusively from the dissolution of the intermetallic layer, the average decrease in layer thickness  $\Delta x_i^d$  is then calculated as described below.

The Nernst-Brunner equation for isothermal dissolution is

$$\ln \frac{C^s - C^0}{C^s - C} = \frac{KAt}{V} \quad (10)$$

where  $C$  is the concentration (atoms per unit volume) of solute in a liquid in contact with a source of solute after a time  $t$  of contact,  $C^0$  is the initial concentration of solute in the liquid, and  $C^s$  is the concentration of solute at saturation.  $A$  is the contact area of the liquid with the solute source,  $V$  is the volume of the liquid and  $K$  is an experimentally determined constant, which normally obeys an Arrhenius relationship of the form

$$K = K^0 \exp\left(-\frac{Q_d}{RT}\right) \quad (11)$$

Here  $K^0$  and  $Q_d$  are experimentally determined Nernst-Brunner parameters.

Assuming constant atomic volume for the liquid, Eq. 10 can be written as

$$\ln \frac{X^s - X^0}{X^s - X} = \frac{KAt}{V} \quad (12)$$

where  $X$  represents the atomic fraction of solute. For the  $i$ th interval Eq. 12 takes the form

$$\ln \frac{X_i^s - X_{i-1}}{X_i^s - X_i} = \frac{KA\Delta t}{V} \quad (13)$$

where  $X_{i-1}$  and  $X_i$  are the atomic fractions of solute in the molten solder at the ends of the  $(i-1)$ th and  $i$ th intervals and  $X_i^s$  is the solubility limit of solute at the temperature  $\bar{T}_i$ . In this paper  $X_i^s$  is given by an equation of the form

$$X_i^s = H^{s0} \exp\left(-\frac{Q_s}{RT_i}\right) \quad (14)$$

where  $X^{s0}$  and  $Q_s$  are parameters determined from experimental data.

Using Eqs. 13 and 14 the atomic fraction  $X_i$  of solute present at the end of any interval is calculated. From it the mass fraction of solute is determined using

$$W_i = \frac{X_i M_{Cu}}{X_i M_{Cu} + (1 - X_i) M_S} \quad (15)$$

where  $M_{Cu}$  is the atomic weight of solute (Cu) and  $M_S$  is the average atomic weight of the solder, which can be assumed constant for practical purposes. From the  $W_i$  values for each interval the mass fraction of solute  $\Delta W_i^d$  dissolved during each interval is determined from

$$\Delta W_i^d = W_i - W_{i-1} \quad (16)$$

and from this the volume  $\Delta V_i^\eta$  of intermetallic ( $\eta$ ) dissolved from the intermetallic layer in each interval is then calculated using

$$\Delta V_i^\eta = \frac{\Delta W_i^d m_s}{W^\eta \rho_\eta (1 - \Delta W_i^d)} \quad (17)$$

In this equation  $m_s$  is the mass of molten solder,  $W^\eta$  is the weight fraction of solute (Cu) in the intermetallic ( $\eta$ ) and  $\rho_\eta$  is the density of the intermetallic. Dividing  $\Delta V_i^\eta$  by the substrate contact area  $A$  then gives the incremental decrease in thickness of the intermetallic layer,

$$\Delta x_i^d = \frac{\Delta V_i^\eta}{A} \quad (18)$$

The increment of layer growth  $\Delta x_i^p$  from precipitation during the  $i$ th interval after saturation (Point S in Fig. 1) is calculated by first determining the average precipitation growth rate  $\bar{v}_i^p$  of the intermetallic layer into the supersaturated intermetallic layer and then multiplying it by the width  $\Delta t$  of the interval. The average growth rate  $\bar{v}_i^p$  is given by

$$\bar{v}_i^p = \frac{-D_i^l}{X_i^s - X^\eta} \frac{X_{i-1}^s - X_i^s}{\delta} \quad (19)$$

where  $X^\eta$  is the atomic fraction of solute in the intermetallic,  $D_i^l$  is the diffusivity of solute in the liquid and  $\delta$  is the thickness of the boundary diffusion layer in the liquid adjacent to the intermetallic.  $D_i^l$  is given by an equation of the form

$$D_i^l = D^{l0} \exp\left(-\frac{Q_l}{RT_i}\right) \quad (20)$$

Thus, the increment of layer growth from precipitation is given by

$$\Delta x_i^p = \frac{D_i^l}{\delta} \left( \frac{X_i^s - X_{i-1}^s}{X_i^s - X^\eta} \right) \Delta t \quad (21)$$

Note that this calculation assumes that the liquid in the diffusion layer of thickness  $\delta$  adjacent to the intermetallic layer becomes incrementally supersaturated with solute during the drop in temperature from  $\bar{T}_{i-1}$  to  $\bar{T}_i$  and that this supersaturation drives the intermetallic incrementally faster by an amount  $\bar{v}_i^p$ .

The program developed to use the above equations to calculate the layer thickening basically has as input an equation or equations for the temperature-

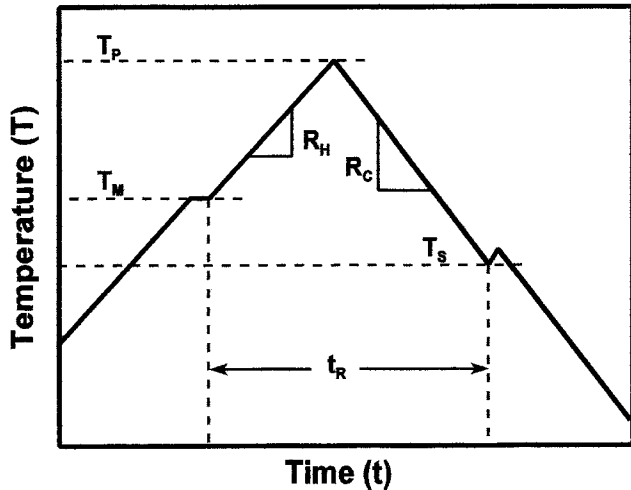


Fig. 2. Schematic diagram of an experimental non-isothermal reflow cycle.  $T_m$  is the melting temperature,  $T_p$  the peak temperature,  $T_s$  the solidification temperature,  $t_r$  the reflow time,  $R_H$  the heating rate, and  $R_C$  the cooling rate.

time profile, the number of intervals, the initial layer thickness and the various experimentally determined growth, dissolution and precipitation parameters. It first calculates  $t_1$  and  $\bar{T}_1$ . Then it calculates and outputs  $\Delta x_i^e$ ,  $\Delta x_i^p$  and  $x_i$ . It then repeats the process for the following intervals until saturation (Point S in Fig. 1) is reached ( $X_i = X_i^s$ ). At this point it starts calculating and outputting  $\Delta x_i^e$ ,  $\Delta x_i^p$ , and  $x_i$ .

**EXPERIMENTAL PROCEDURE**

**Materials and Soldering Procedures**

Solder paste containing 96.5wt.%Sn and 3.5wt.%Ag solder in a mildly activated rosin (RMA) flux as well as bulk solder of the same composition were used to prepare the various samples used. These materials were reflow soldered on 1 mm thick 99.9wt.%Cu sheet specimens of various sizes. All copper sheet specimens were cleaned in a solution of equal parts by volume of nitric, acetic and phosphoric acids and rinsed in water and methanol prior to soldering.

For studies of the isothermal growth of the intermetallic layer between molten solder and Cu substrate at temperatures ranging from 500 K (226°C) to 565 K (292°C), 10 mm × 5 mm × 1 mm Cu substrates were first preheated to the desired reflow temperature on a Dataplate Series 730 programmable hot plate, with the temperature-time profile being monitored by a dummy Cu specimen that had a fine gage chromel-alumel thermocouple imbedded in an appropriate amount of solder on it. After the specimen had attained the reflow temperature, a small amount of activated rosin (AR) flux was added to break up an oxide layer, and then, after waiting an additional 30 seconds for the temperature of the specimen to recover a fixed amount of solder paste (≈0.1 g) was applied with an EFD 1000 DV-SMT dispenser. The resulting Cu area to solder volume ratio was approximately 3.7 mm<sup>2</sup>/mm<sup>3</sup>. The solder paste spread over the Cu substrate immediately and melting occurred within a few seconds. The time at which melting occurred was taken as the start time for intermetallic growth. Reflow temperatures ranged from 20 to 480 seconds. After reflow was complete specimen were quenched on a steel block.

For studies of the isothermal dissolution of Cu in molten solder using a Nernst-Brunner analysis (Eq. 10) at 527 K (254°C), 545 K (272°C), and 575 K (302°C), 10 mm × 10 mm × 1 mm Cu substrates were reflow soldered as described above for 60, 120, and 240 s. However, instead of solder paste, 0.2 and 0.4 mm thick pieces of solder sheet 10 mm × 10 mm were used. This gave two different volumes of solder. After soldering, the substrate contact area was measured and the solder volume was determined by weighing the sample and subtracting the weight of the Cu substrate. Thus, for each temperature six different At/V values were available for determining K in Eq. 10.

For determining the solubility limits of Cu in molten solder at temperatures ranging from 303 K (230°C) to 573 K (300°C), 10 mm × 10 mm × 1 mm Cu substrates were reflow soldered isothermally with 10 mm × 10 mm × 0.5 mm pieces of solder. The solder and

**Table I. Reflow Parameters for Non-Isothermal Reflow Samples\***

Specimen Number	$T_M$ (K)	$T_P$ (K)	$T_S$ (K)	$R_H$ (K/min)	$R_C$ (K/min)	$T_R$ (min)
<b>Programmable Oven Method</b>						
1	491	513	476	5.6	4.4	13.8
2	492	536	477	5.6	4.8	21.7
3	491	514	475	5.6	39.8	5.0
4	492	535	475	5.6	37.9	10.4
<b>Hot Plate, Cu Block Quench Method</b>						
5	493	514	483	5.6	620	3.1
6	490	534	477	5.6	1210	8.5

\*The meaning of symbols in the table are given in Fig. 2.

substrate were coated with an RMA flux and then reflowed in either a VWR Scientific 1330 FM convection oven or a Lindberg muffle furnace for either 5 or 10 h. Based on the Nernst-Brunner dissolution studies it was known that 5 h was sufficient to guarantee saturation of the solder with Cu. The actual reflow temperatures were measured with a thermocouple located near the specimens.

For the study of intermetallic layer growth under non-isothermal conditions, six 10 mm × 5 mm × 1 mm Cu specimens were used. After cleaning the Cu substrates, approximately 0.1 g of solder paste was dispensed on them with an EFD 1000 DV-SMT dispenser. These specimens were then heated to peak reflow temperatures of either 513 K (244°C) or 535 K (262°C) at a rate of 5.6°/min on either a Dataplate Series 730 programmable hot plate or in a Despatch 924D forced convection oven equipped with a DRP-13 digital rate controller and using CO<sub>2</sub> as a coolant. The specimens were cooled from the peak reflow temperatures at rates ranging from 4.4°/min to 1210°/min. The faster cooling rates were attained by quenching on a Cu block from the hot plate and, and the slower rates were attained by controlled cooling in the convection oven. All temperature-time profiles were followed with a fine gage chromel-alumel thermocouple in a dummy specimen and a strip chart recorder. A schematic diagram of a non-isothermal reflow cycle is shown in Fig. 2, and Table I gives the associated reflow parameters.

### Metallography

Specimens for the determination of the average intermetallic layer thickness were sectioned perpendicular to the solder/substrate interface with a Buehler Isomet low speed saw with a high concentration diamond wafering blade. These cross sections were then mounted in epoxy, ground through 1200 SiC paper and polished with 6 μm and 1 μm diamond paste on a Buehler Texmet polishing cloth. After cleaning ultrasonically in de-ionized water, final polishing was done using Buehler Mastermet colloidal silica solution on a Buehler Chemomet polishing cloth. The polished specimens were then rinsed in de-ionized water and methanol, dried, and etched in a solution of 2.5% HNO<sub>3</sub> and 1% HCL in methanol for 2 s to 5 s.

Light micrographs of the intermetallic layer for determinations of the average intermetallic layer thickness were obtained at X1,500 using a B&L Research Metallograph with an X85 oil immersion objective, with a stage micrometer being used to check the magnification. Photomicrographs were obtained from three representative areas near the center of the specimen, and the average thickness of the layer in each micrograph was obtained by dividing the area occupied by the intermetallic layer by its length and the magnification. The area occupied by intermetallic layer was obtained from scanned images of the photomicrographs using NIH Image, Version 1.59 image analysis software. The area of the total intermetallic layer, including both ε and η phases, was determined.

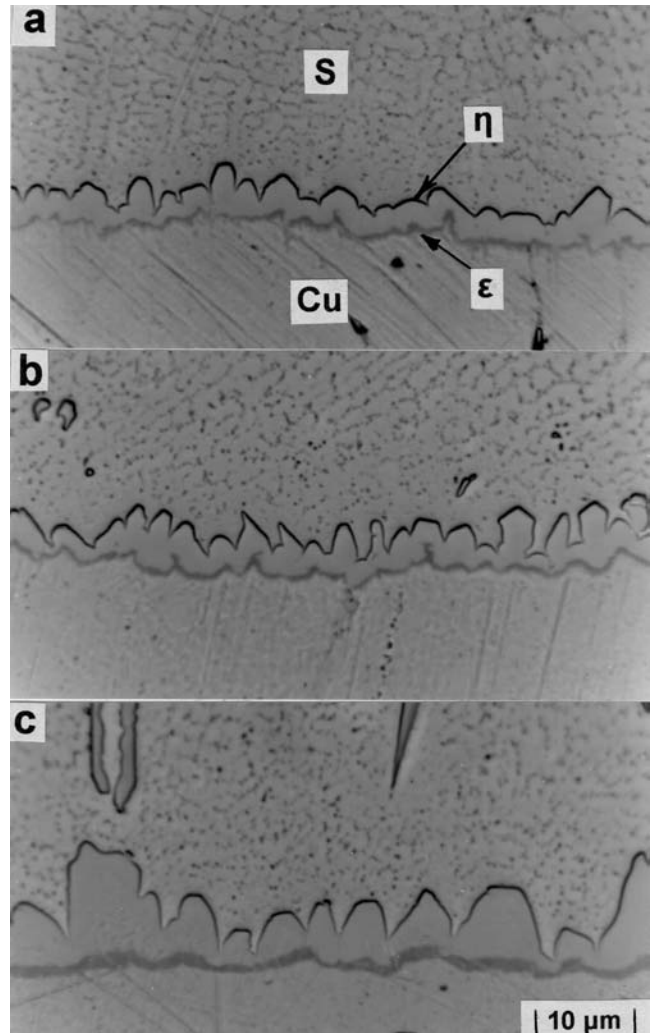


Fig. 3. Microstructures of the intermetallic layers ( $\eta$  and  $\epsilon$ ) formed between molten Sn-3.5Ag solder S and Cu during 8 minute isothermal reflows at (a) 499 K (226°C), (b) 524 K (251°C), and (c) 565 K (292°C) showing that the layer consists of scalloped  $\eta$  phase grains and thin continuous layer of  $\epsilon$  phase.

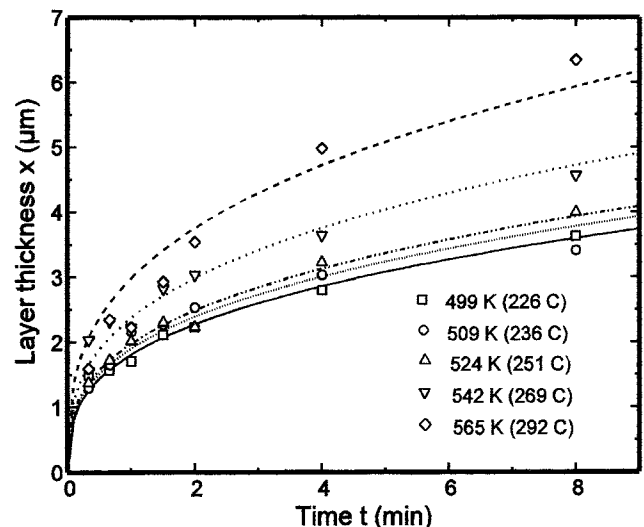


Fig. 4. Average intermetallic layer thickness  $x$  resulting from isothermal reflow at various temperatures as a function of reflow time  $t$ . Curves represent fits of the data with the equation  $x = kt^{0.33}$ .

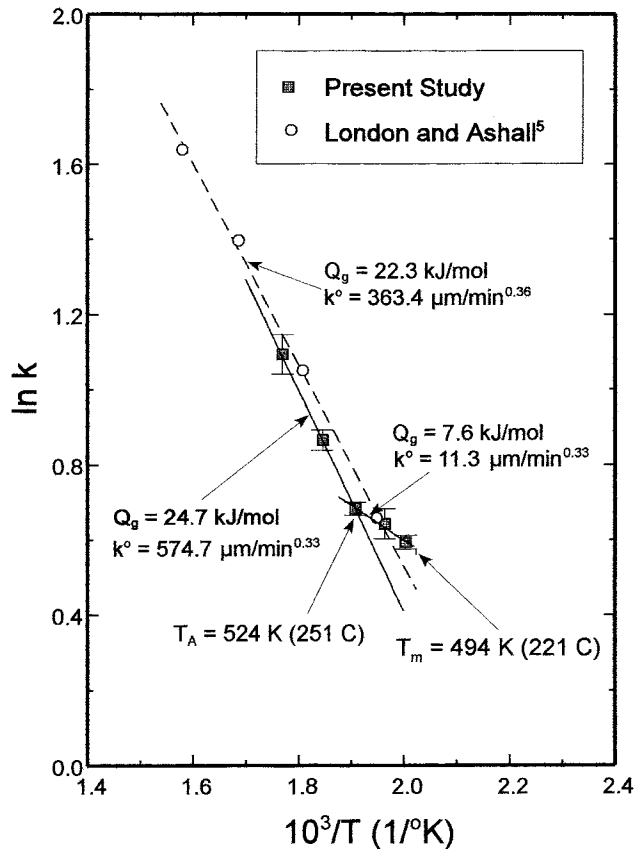


Fig. 5. Arrhenius plot of  $k$  values obtained from the curve fits in Fig. 4 and from London and Ashall<sup>5</sup>. The straight line fits above and below the transition temperature  $T_A$  represents fits of the data with Eq. 5.

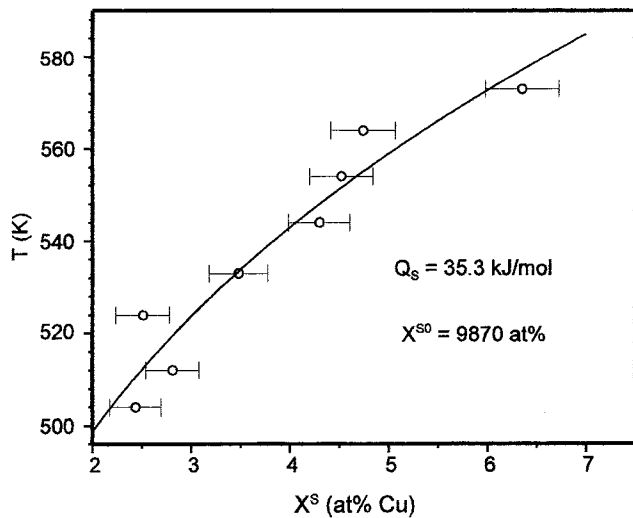


Fig. 6. Energy dispersive spectroscopy (EDS) measurements of the average Cu content in solder saturated with Cu at various temperatures. The curve represents a fit of the data with the equation  $X^S = X^{S0} \exp(-Q_S/RT)$ .

### Microanalysis

The average Cu concentration in the solder of dissolution and solubility limit study specimens was determined by energy dispersive spectroscopy (EDS) with a NORAN Series II analyzer on a JEOL JSM 35 scanning electron microscope operated at 25 kV. The

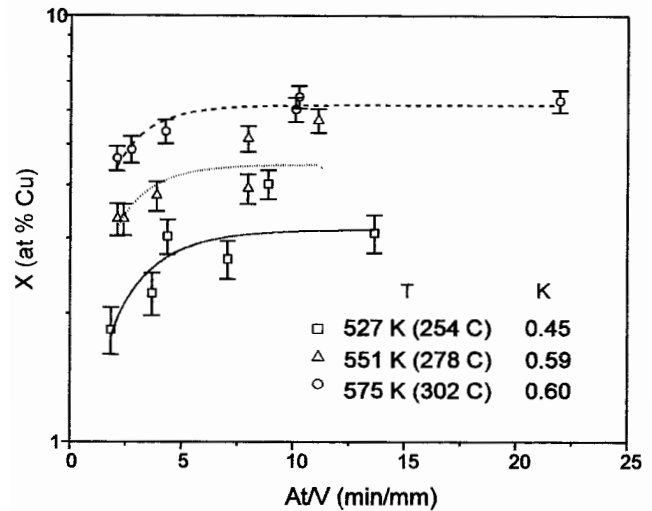


Fig. 7. Energy dispersive spectroscopy (EDS) measurements of the average Cu content of isothermally reflowed specimens having two different substrate surface area ( $A$ ) to solder volume ( $V$ ) ratios and reflowed for 60, 120, and 240 seconds. The curves represent fits of the Nernst-Brunner equation (Eq. 12) to the data. The  $K$  values are those obtained from the curve fits.

background and ZAF corrected relative integrated intensity ratios of the  $\text{Cu } K\alpha$ ,  $\text{Sn } L\alpha$ , and  $\text{Ag } L\alpha$  peaks were obtained from three areas on each specimen scanned at X50 for 200 s using the NORAN SSQ program. The atomic percent Cu for each analysis was obtained from a calibration curve relating relative intensity ratios to Cu content. This curve was established using solder standards containing 0 wt.%, 1 wt.%, 2 wt.%, 3 wt.%, and 4 wt.% Cu. All specimen surfaces were ground through 600 grit paper prior to analysis.

## RESULTS AND DISCUSSION

### Isothermal Growth of Intermetallic Layer into Molten Solder

As expected the thickness of the intermetallic layer increased with increasing time at each reflow temperature and with increasing temperature for each reflow time. Qualitatively the microstructure for all reflow temperatures and times was the same. That is, it consisted of scalloped grains of  $\eta$  ( $\text{Cu}_6\text{Sn}_5$ ) phase with deep grooves between them in contact with the molten solder and a thinner continuous layer of  $\epsilon$  ( $\text{Cu}_3\text{Sn}$ ) phase between the  $\eta$  phase and the Cu substrate (Fig. 3). The grain size of the  $\eta$  phase also increased with increasing reflow temperature and time. This morphology is typical of intermetallic layers formed between molten Sn containing solders and Cu substrates.<sup>4</sup>

As can be seen in Fig. 4 the average total ( $\eta + \epsilon$ ) intermetallic layer thickness  $x$  increases monotonically with increasing reflow time, with the rate of increase decreasing with time. The data for each of the five reflow temperatures were initially least squares fitted with curves of the form  $x = kt^n$  to determine the parameters  $k$  and  $n$ . These five fits showed that the  $n$  values averaged  $0.33 \pm 0.07$ . Since

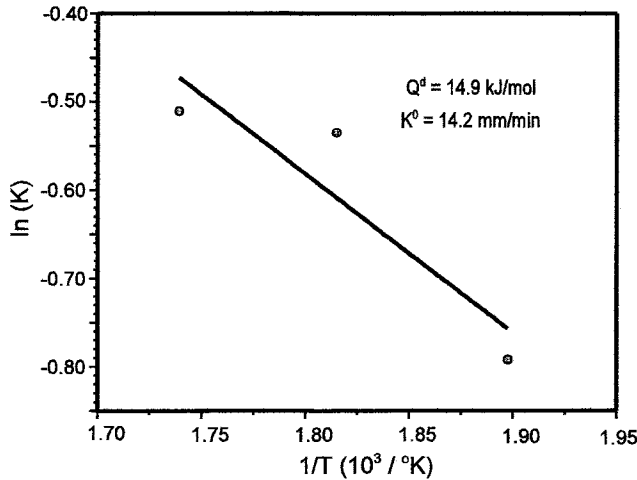


Fig. 8. Arrhenius plot of the Nernst-Brunner  $K$  values obtained from curve fits of the data in Fig. 7. The straight line represents a fit of the data with Eq. 11.

$n = 0.33$  has some theoretical basis<sup>4</sup> a second fitting of the data was made using  $x = kt^{0.33}$ . These fits yielded the  $k$  values shown in the Arrhenius plot in Fig. 5. As can be seen the data agree well with that of London and Ashall,<sup>5</sup> who used much longer reflow times. The data in the present study does, however, exhibit a deviation from linearity. Thus, rather than fit the data with a single straight line of the form of Eq. 5, it was fit with the two lines shown in the figure. Thus, in applying the numerical method one set of  $Q_s$  and  $k^0$  values were used above the transition temperature  $T_A$  and another below it. These are the values given in the figure. No explanation lends itself presently to the non-linearity. As can be seen in Fig. 3 there is no difference in microstructure above and below  $T_A$ , indicating that the mechanisms of layer growth above and below it are the same.

### Isothermal Dissolution

Figures 6 and 7 show the results of EDS measurements of the average amount of Cu dissolved in molten solder at saturation and under various conditions short of saturation, respectively. The solubility temperatures given in Fig. 6 are 50°C to 100°C below the reported liquidus temperatures for the  $\eta + \text{liquid}$  phase field in the binary Cu-Sn system. This is expected in that 3.5wt.%Ag is expected to lower the equilibrium temperatures for the equilibrium between  $\eta$  and liquid. The data were fit with an Arrhenius equation of the form,  $X^S = X^{S0} \exp(-Q_s/RT)$ , to give the parameters  $Q_s$  and  $X^{S0}$  needed by Eq. 14 of the numerical method.

The dissolution data in Fig. 7 show that the atomic fraction of dissolved Cu increases and then levels off with an increase in the Nernst-Brunner parameter  $At/V$ . These isothermal sets of data were fit with the Nernst-Brunner equation (Eq. 12) to obtain the curves in the figure. Values of  $X^S$  from the curve fit to the solubility data in Fig. 6 were used in making these curve fits. The curve fits in Fig. 7 yielded the values of  $K$ , the Nernst-Brunner dissolution rate constant,

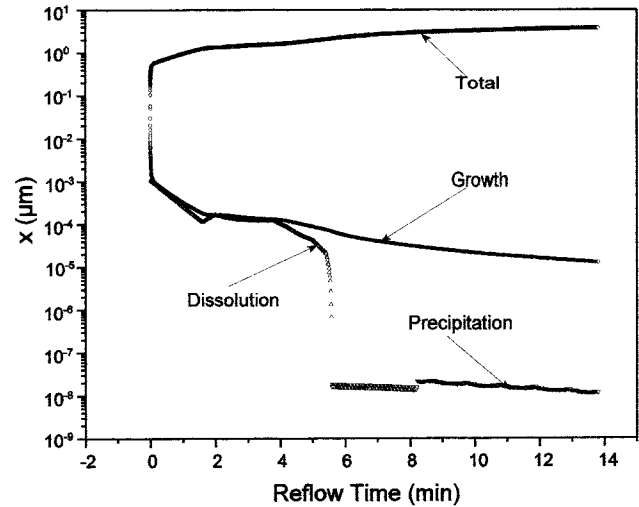


Fig. 9. Plot of individual contributions to the layer thickness from growth  $\Delta x_i^g$ , dissolution  $\Delta x_i^d$  (negative value) and precipitation  $\Delta x_i^p$  for selected isothermal intervals along with the total intermetallic layer thickness  $x$  as a function of reflow time for the temperature-time profile for Specimen 1 in Table I.

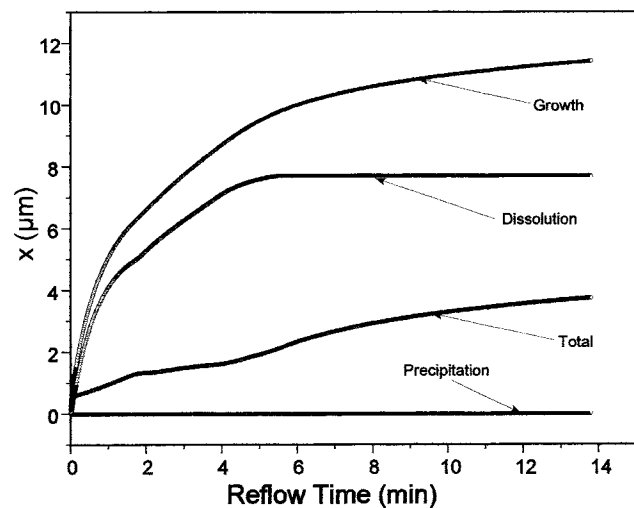


Fig. 10. Plot of the cumulative values of individual contributions to the layer thickness from growth  $\Sigma \Delta x_i^g$ , dissolution  $\Sigma \Delta x_i^d$  (negative value) and precipitation  $\Sigma \Delta x_i^p$  along with the total intermetallic layer thickness as a function of reflow time for the temperature-time profile for Specimen 1 in Table I.

presented in the Arrhenius plot in Fig. 8. These three data points were, in turn, fit with a straight line to yield the parameters  $Q_d$  and  $K^0$  needed by Eq. 11 of the numerical method.

### Non-isothermal Growth of Intermetallic Layers

Morphologically the growth of the intermetallic layers during the non-isothermal reflow cycles given in Table I is the same as that for growth under isothermal conditions. That is, the microstructures at the end of aging were the same as those shown in Fig. 3. The average thicknesses of the layers formed by these non-isothermal cycles were determined and compared with values calculated with a FORTRAN program based on the numerical method presented previously.

**Table II. Output for the Numerical Method for Non-Isothermal Reflow of Specimen 1 in Table I**

Interval Number	$\bar{T}_i$ (K)	$\Delta x_i^g$ ( $\mu\text{m}$ )	$\Delta x_i^d$ ( $\mu\text{m}$ )	$\Delta x_i^p$ ( $\mu\text{m}$ )	$\sum \Delta x_i^g$ ( $\mu\text{m}$ )	$\sum \Delta x_i^d$ ( $\mu\text{m}$ )	$\sum \Delta x_i^p$ ( $\mu\text{m}$ )	$\Delta x_i$ ( $\mu\text{m}$ )
1	491	$5.73 \times 10^{-2}$	$0.11 \times 10^{-2}$	0.00	$5.73 \times 10^{-2}$	$0.11 \times 10^{-2}$	0.00	$5.62 \times 10^{-2}$
1,000	491	$9.35 \times 10^{-5}$	$8.76 \times 10^{-4}$	0.00	1.56	0.97	0.00	0.59
36,229	513	$8.68 \times 10^{-5}$	$4.10 \times 10^{-5}$	0.00	9.48	7.57	0.00	1.91
39,126	513	$7.37 \times 10^{-5}$	$2.02 \times 10^{-5}$	0.00	9.71	7.66	0.00	2.05
40,000	513	$6.95 \times 10^{-5}$	$5.76 \times 10^{-6}$	0.00	9.78	7.67	0.00	2.11
40,430	513	$6.73 \times 10^{-5}$	0.00	$1.61 \times 10^{-8}$	9.81	7.67	$1.61 \times 10^{-8}$	2.14
49,995	508	$4.05 \times 10^{-5}$	0.00	$1.68 \times 10^{-8}$	10.30	7.67	$1.57 \times 10^{-4}$	2.63
60,000	503	$2.92 \times 10^{-5}$	0.00	$2.08 \times 10^{-8}$	10.65	7.67	$3.10 \times 10^{-4}$	2.98
80,000	490	$1.80 \times 10^{-5}$	0.00	$1.60 \times 10^{-8}$	11.10	7.67	$6.79 \times 10^{-4}$	3.43
99,990	476	$1.26 \times 10^{-5}$	0.00	$1.15 \times 10^{-8}$	11.41	7.67	$9.47 \times 10^{-4}$	3.74

**Table III. Summary of the Predicted and Measured Layer Thickness Values for the Non-Isothermal Specimens**

Specimen Number	Layer Thickness ( $\mu\text{m}$ )	
	Measured	Predicted
1	$4.76 \pm 0.45$	3.74
2	$8.22 \pm 0.70$	4.48
3	$3.34 \pm 0.34$	2.36
4	$4.80 \pm 0.30$	2.72
5	$1.96 \pm 0.48$	1.61
6	$2.62 \pm 0.18$	1.98

The numerical method was used to evaluate the non-isothermal growth of layers by first inputting appropriate values for the various parameters in the relevant equations presented in the Numerical Method section as well as by inputting values for the melting temperature ( $T_M$ ), peak temperature ( $T_p$ ), solidification temperature ( $T_s$ ), heating rate ( $R_H$ ) and cooling rate ( $R_c$ ) from Table I to the program. Some of the parameters ( $k^0$ ,  $Q_g$ ,  $T_A$ ,  $X^{S0}$ ,  $Q_s$ ,  $K^0$  and  $Q_d$ ) are the experimentally determined values presented in previous sections. Others such as the substrate area  $A$  and the solder volume  $V$  were established for each sample. Still others were taken from the literature.  $D^{10}$  and  $Q_i$  in Eq. 20 were taken to be the values ( $1.08 \text{ cm}^2 \text{ s}^{-1}$  and  $17.6 \text{ kJ mol}^{-1}$ , respectively) given by Ma and Swalin<sup>6</sup> for the diffusion of Cu in pure liquid Sn. The boundary layer thickness  $\delta$  in Eq. 21 was assumed to be  $50 \mu\text{m}$  based on the work of Forgens and Grace.<sup>7</sup>

To start the calculation the reflow time  $t_R$  was divided into 100,000 intervals and an initial intermetallic layer thickness of  $x_0 = 0$  was assumed. The program then calculated values of  $\Delta x_i^g$ ,  $\Delta x_i^p$  and  $\Delta x_i$  (Eq. (3a)) until saturation of the liquid by Cu was attained  $X_i = X_i^s$ . After this interval the program began calculating  $\Delta x_i^d$ ,  $\Delta x_i^p$  and  $x_i$  (Eq. 3b). This continued until solidification.

Figure 9, Fig. 10, and Table II present the output of the program for the reflow cycle seen by Specimen 1 in Table I. As can be seen in Fig. 9 and Table II the numerical method predicts that incremental contributions to intermetallic thickening from the isother-

mal growth term  $\Delta x_i^g$  drop off rapidly from  $5.73 \times 10^{-2} \mu\text{m}$  for the 1<sup>st</sup> time interval to  $8.76 \times 10^{-4} \mu\text{m}$  for the 1,000<sup>th</sup> interval. Thereafter the contribution decreases slowly for the remaining 99,000 cycles. The negative contribution of the dissolution increments to thickening  $\Delta x_i^d$  initially follow the positive incremental increases from growth but are always somewhat smaller, thus guaranteeing a net increase in layer thickness  $x_i$  with increasing reflow time. After 5 minutes ( $i \sim 36,000$ ) the incremental contributions from dissolution start to drop off rapidly. This rapid drop off seems to be associated with the passing of the peak temperature  $T_p$  and the start of the cooling part of the reflow cycle.  $T_p$  for Specimen 1 is attained after 3.9 minutes. After cooling begins saturation should be approached rapidly. After passing the point of saturation at about 5.6 minutes of 40,000 increments, dissolution no longer contributes to overall growth and the precipitation term  $\Delta x_i^p$  in Eq. 3b starts to contribute. As can be seen in Fig. 9 and Table II its contribution to overall growth is very small and for practical purposes can be neglected.

Figure 10 shows the cumulative contributions to growth from  $\Delta x_i^g$ ,  $\Delta x_i^d$  and  $\Delta x_i^p$  as well as the net layer thickness  $x_i$  predicted for Specimen 1 as a function of reflow time on a linear scale. Again it is seen here that  $\Delta x_i^g$  and  $\Delta x_i^d$  are the main contributors to the overall growth of the layer. Table III presents values for the measured average thickness of intermetallic layers found to have been formed during the six reflow treatments in Table I as well as values calculated by the numerical method. As can be seen the numerical method under predicts the layer thickness for all specimens. The authors feel that the main reason for this is associated with the values of  $k^0$  and  $Q_g$  used to calculate the  $\Delta x_i^g$  values. The values of  $k^0$  and  $Q_g$  were obtained from isothermal growth experiments in which the molten solder was not saturated prior to the start of the formation of the intermetallic layer. Schaefer et al.<sup>2</sup> have shown that isothermal growth of intermetallic into molten near eutectic Sn-Pb-Ag solder is considerably faster for growth into saturated solder.

#### ACKNOWLEDGEMENTS

The authors gratefully acknowledge Visteon Automotive Systems for supporting this work. Also, one of



the authors, W. Laub, wishes to express his gratitude to the Alexander von Humboldt Foundation for their support during the course of the study.

#### REFERENCES

1. M. Schaefer, W. Laub, J.M. Sabee, and R.A. Fournelle, *J. Electron. Mater.* 25, 992 (1996).
2. M. Schaefer, W. Laub, R.A. Fournelle, and J. Liang, *Design and Reliability of Solders and Solder Interconnects*, ed. R.K. Mahidhara et al., (Warrendale, PA: TMS, 1997), p. 247.
3. D.A. Porter and K.E. Easterling, *Phase Transformations in Metals and Alloys* (Berkshire, England: Van Nostrand Reinhold, 1981), p. 213.
4. M. Schaefer, R.A. Fournelle, and J. Liang, *J. Electron. Mater.* 27, 1167 (1998).
5. J. London and D.W. Ashall, *Brazing and Soldering* 11, 49 (1986).
6. C.H. Ma and R.A. Swalin, *Acta Metall.* 8, 388 (1960).
7. W.D. Forgeng, Jr. and R.E. Grace, *Trans. AIME* 242, 1249 (1968).